

Available online at [www.sciencedirect.com](http://www.sciencedirect.com)

Procedia Computer Science 4 (2011) 938–947

---

**Procedia**  
Computer Science

---

International Conference on Computational Science, ICCS 2011

# Model Reduction Techniques for Characterization of Fractured Subsurfaces

Victor Ginting<sup>a,\*</sup>, Michael Presho<sup>b</sup><sup>a</sup>*Department of Mathematics, University of Wyoming, Laramie, Wyoming, USA*<sup>b</sup>*Department of Mathematics, Colorado State University, Fort Collins, Colorado, USA*

---

## Abstract

One of the most difficult tasks in reservoir simulations is reliable characterization of fractured subsurfaces. A typical situation in petroleum engineering employs dynamic data integrations such as the oil production history to be matched with simulated responses associated with a set of porosity and/or permeability fields. Among the challenges found in practice are proper mathematical modelings of the flow in the presence of fractured systems, persisting heterogeneity in the porosity and permeability, and the uncertainties inherent in them. In this paper we propose a Bayesian framework Monte Carlo Markov Chain simulation (MCMC) to sample a set of subsurface's characteristics from the posterior distribution that are conditioned to the production data. This process requires obtaining the simulated responses over many realizations. The flow for this simulated response is governed by a dual porosity, dual permeability model. As this can be a prohibitively expensive endeavor, we address the possibility of using the Multi-scale Finite Volume Element (MsFVEM) combined with a sparse stochastic collocation technique to provide a venue for an efficient computation. A set numerical examples illustrating the procedure will be presented.

**Keywords:** fractured reservoir, uncertainty quantification, Bayesian statistics, MCMC, multiscale finite volume element, stochastic collocation

---

## 1. Introduction

Reliable characterization of fractured subsurfaces is one of the most challenging tasks in the flow through porous media community. Many reservoirs are naturally fractured and can contain fractures that may span over many length scales. The fractures give rise to very complex paths for the fluid movement which directly affect subsurface characterization. A common practice in the hydrocarbon recovery industry is to use the available production data to guide the characterization of a particular reservoir. This practice, which is coined “history matching,” amounts to adjusting the reservoir model until it closely reproduces the recorded production data. In reality, history matching requires sampling the subsurface's characteristics, such as porosity and permeability fields, submitting them as input parameters to the reservoir model (usually expressed in terms of a set of governing mathematical principles), obtaining the output of simulated responses, and then comparing them with the measured data.

---

\*Corresponding Author

Email address: [vginting@uwyo.edu](mailto:vginting@uwyo.edu) (Victor Ginting)

However, direct simulations of flow through fractured reservoirs may be computationally expensive or infeasible to compute. Ideally, the level of mesh resolution on which the flow and transport are sought has to be in a comparable scale with the fractures' setting. Often this would require designing a highly unstructured grid along with the possibility of local refinements in various subregions. Moreover, a great deal of prior information about the fracture configuration must be gathered for constructing such a grid system. Putting this into the scenario of sampling large numbers of reservoir characteristics, one can see the tremendous computational load that has to be committed in the history matching.

On a related aspect, it is not immediately obvious how to rigorously represent the subsurface characteristics before sending them to the reservoir model. In this regard, the predicament lies on the uncertain nature of these characteristics. In our context, the values of these characteristics have to be projected to the underlying computational mesh on which the simulated responses are to be evaluated. This will translate into the dimensional immensity of the uncertainty space which greatly multiplies the already huge computational cost.

To recapitulate, establishing a complete statistical description of the fracture subsurface that is consistent with the production data necessitates focusing the effort on addressing three fundamental problems, namely, (1) proper modeling of the flow and transport in a fractured subsurface, (2) appropriate parametrization of the subsurface's characteristics in hopes of representing the uncertainty correctly, and (3) accurate numerical procedures that make the overall computational work tractable. Our thesis in this paper is that these fundamental problems can be resolved by implementing careful modeling reduction techniques. The reduced system is then placed as a blackbox in the framework of Bayesian statistical inference in combination with the Markov chain Monte Carlo (MCMC) method. This statistical approach aims at generating a Markov chain from which a stationary, posterior distribution of the fracture characteristics may be constructed [11]. In our case, the goal is to describe the posterior distribution of the permeability conditioned to known tracer cut data.

Since our goal is to mimic the behavior of integrated dynamic responses such as the production data, it is likely satisfactory to use relatively inexpensive surrogate mathematical models that are capable of predicting the general trends of the flow and transport in the fractured subsurface. This is the first step in the sequence of modeling reductions that we propose in this paper. One suitable candidate is the class of dual porosity and dual permeability models whose initial inception originally appeared in the literature in the 1960's and 1970's, see e.g. [3, 17, 13]. Typical assumptions in fractured reservoir simulation are that the permeability within the fracture set is noticeably larger than its matrix counterpart, and that fractures represent the main means of fluid transport in a porous medium. More recent investigations attempted to provide rigorous derivations of the dual models using the mathematics of homogenization theory (see [1, 2, 8]). Effectively modeling such systems typically involves solving for equations which govern flow in the matrix and fracture separately and maintaining a certain interconnection between the two.

Furthermore, as the uncertainty space of a permeability field may be exceptionally large, a reduction of the space dimension is a step which must be performed for computationally feasible simulations. The well known Karhunen-Loève expansion allows us to parametrize our random space and thereby lead to the desired reduction. The parametrization is achieved by solving an eigenvalue problem involving a given covariance structure and the assumption of uncorrelated random coefficients. This technique has been used previously in flow through porous media applications (see, e.g. [9, 10]), where a random permeability field defined on a large number of underlying grid points is expressed using the expansion.

The last straw concerns the numerical procedures for solving the dual model. The main burden when solving this surrogate model is dominated by the coupled pressure equations (see Eq. (1) in Section 2). This mostly stems from the heterogeneous nature of the permeabilities associated with the fracture and matrix sheets. We propose to employ the Multiscale Finite Volume Element method (MsFVEM) to solve the coupled pressure equation for two main reasons: (1) the finite volume framework enjoys a local numerical conservation, which is a crucial property for an accurate simulation of transport phenomena, and (2) the method allows for a degree of freedom reduction in the resulting algebraic systems by posing the calculation on a coarser mesh and representing the approximate solutions in terms of the multiscale basis functions. The multiscale basis functions are designed in such a way that they contain information about the heterogeneity of the permeabilities. Still, in terms of large scale permeabilities sampling, the cost for recalculation of these basis functions can easily be extremely expensive. Rather than resolving the multiscale basis functions for every permeability realization, we propose to use the sparse interpolation technique [16]. A set of collocation points in the parametrized uncertainty space is chosen on which the multiscale basis functions are computed prior to the MCMC iterations. Then within MCMC, everytime a proposal for the permeabilities are made,

the associated multiscale basis functions are computed in terms of stochastic interpolation of those precomputed counterparts at the collocation points. We note that similar approach has been implemented in [6] and [7].

The rest of the paper is organized as follows. Section 2 lays out the dual model that serves as a surrogate governing principle for the flow and transport in fractured subsurface. Section 3 gives a description on the Karhunen-Loève expansion to parametrize the uncertainty space. Then in Section 4 we present the MsFVEM followed by the stochastic interpolation technique in Section 5. The MCMC algorithm is presented in Section 6. A set of numerical simulations is shown in Section 7. Finally we offer a concluding remark in Section 8.

## 2. Dual porosity, dual permeability flow model

This section describes the surrogate model we use for characterizing the reservoir in the MCMC framework. We employ the dual porosity, dual permeability model for single-phase (tracer) flow through a fractured porous medium, denoted by  $\Omega$ , see e.g. [3, 17, 13]. Other recent models, such as in [1, 2, 8], are already available. Nevertheless, in the interest of focusing our effort on developing the general MCMC framework for fractured reservoirs we will use the more traditional models in [13]. We expect that as our level of understanding matures, exchange of these models is achievable.

The basic idea of such models is separation of the matrix and fracture equations which describe flow through the system while maintaining the interaction between the two by an additional transfer term. The equations governing the pressures are expressed as

$$\frac{\alpha k_m(x, \omega)}{\mu} (p_m - p_f) - \nabla \cdot \left( \frac{k_m(x, \omega)}{\mu} \nabla p_m \right) = q_{m,p} \quad \text{and} \quad -\frac{\alpha k_m(x, \omega)}{\mu} (p_m - p_f) - \nabla \cdot \left( \frac{k_f(x, \omega)}{\mu} \nabla p_f \right) = q_{f,p}, \quad (1)$$

where  $\mu$  denotes the viscosity of the tracer, and  $k_m$  and  $k_f$  denote the matrix and fracture permeabilities, respectively, which change with different points  $x \in \Omega$ . The uncertainty inherent in the permeabilities is indicated by  $\omega$ . The variables  $p_m$  and  $p_f$  denote the respective pressures. The forcing terms  $q_{m,p}$  and  $q_{f,p}$  denote the matrix and fracture sources and sinks, respectively. It is evident from the equations that the coupling in the system is realized through the matrix-fracture transfer function  $\frac{\alpha k_m}{\mu} (p_m - p_f)$ , where  $\alpha$  is referred to as the shape factor. In this paper we assume a shape factor of the form  $\alpha = \frac{s}{L_z^2}$ , where  $L_z$  denotes the vertical fracture spacing, and  $s$  is the shape factor coefficient. We note that shape factors and applicable shape factor coefficients are a topic in the previous research, and we refer the interested reader to [13, 17] for details of extensive discussion on the proper use of transfer terms.

Along with the dual permeability pressure equations given in (1) the flow model also involves two tracer concentration equations given by

$$\phi_m \frac{\partial C_m}{\partial t} + \nabla \cdot (\mathbf{v}_m C_m) - \Gamma_c = q_{m,c} \quad \text{and} \quad \phi_f \frac{\partial C_f}{\partial t} + \nabla \cdot (\mathbf{v}_f C_f) + \Gamma_c = q_{f,c}, \quad (2)$$

where

$$\mathbf{v}_m = -\frac{k_m}{\mu} \nabla p_m \quad \text{and} \quad \mathbf{v}_f = -\frac{k_f}{\mu} \nabla p_f \quad (3)$$

are the velocities gained from (1),  $\phi_m$  and  $\phi_f$  denote the matrix and fracture porosities,  $q_{m,c}$  and  $q_{f,c}$  are the corresponding forcing terms for each equation, and  $C_m$  and  $C_f$  denote the respective tracer concentrations. The concentration matrix-fracture exchange term  $\Gamma_c$  depends on the difference of matrix and fracture pressures and is determined by [14]

$$\Gamma_c(x, t) = \begin{cases} -\frac{\alpha k_m}{\mu} (p_m(x) - p_f(x)) C_m(x, t) & \text{if } p_m(x) \geq p_f(x), \\ -\frac{\alpha k_m}{\mu} (p_m(x) - p_f(x)) C_f(x, t) & \text{if } p_m(x) < p_f(x). \end{cases} \quad (4)$$

A heuristic consideration verifies this form, as flow from the matrix to fracture (or vice-versa) would result from a pressure difference across the respective domains.

Our goal in this paper is to sample the fine scale permeability fields  $k_m$  and  $k_f$  on the basis of the tracer fractional flow. That is, we are interested in the fraction of tracer produced with respect to the total production rate. The tracer fractional flow (or tracer cut),  $F(t)$ , is defined by the flow rate at the production edge of the model given by

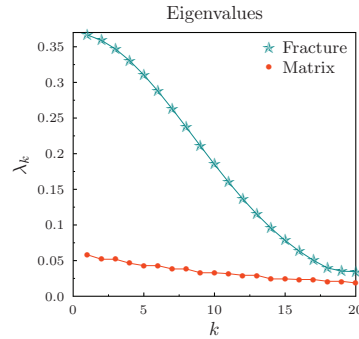


Figure 1: Eigenvalues decrease in the KLE expansion

$$F(t) = \frac{\int_{\partial\Omega^{\text{out}}} \mathbf{v}_f \cdot \mathbf{n} C_f dl + \int_{\partial\Omega^{\text{out}}} \mathbf{v}_m \cdot \mathbf{n} C_m dl}{\int_{\partial\Omega^{\text{out}}} (\mathbf{v}_f + \mathbf{v}_m) \cdot \mathbf{n} dl}, \quad (5)$$

where  $\partial\Omega^{\text{out}}$  is the outflow boundary and  $\mathbf{n}$  is the unit normal vector on  $\partial\Omega^{\text{out}}$ . We refer to  $F(t)$  as the composite tracer cut curve.

In practice, the permeability within the fracture system,  $k_f$ , is larger than its matrix counterpart,  $k_m$ . In addition we assume  $\phi_f < \phi_m$  to account for less storage capacity of the fractures. In turn, the flow patterns of the fracture advance significantly faster in time, and strongly affect the flow scenario for the Markov chain Monte Carlo (MCMC) process.

### 3. Parametrization of uncertainty in the permeabilities

To proceed with parametrizing the uncertainty space, the prior information of the matrix and fracture permeabilities is assumed to follow a log-normal distribution. That is,  $\log(k_m(x, \omega)) = Y_m(x, \omega)$  and  $\log(k_f(x, \omega)) = Y_f(x, \omega)$ , where  $Y_m(x, \omega)$  and  $Y_f(x, \omega)$  follow Gaussian distribution with covariance function

$$R_s(x_1, z_1; x_2, z_2) = \sigma_s^2 \exp\left(-\frac{|x_1 - x_2|^2}{2l_{x,s}^2} - \frac{|z_1 - z_2|^2}{2l_{z,s}^2}\right), \quad (6)$$

where  $l_{x,s}$  and  $l_{z,s}$  denote the correlation lengths,  $\sigma_s^2$  is the variance, and  $s$  signifies either matrix ( $m$ ) or fracture ( $f$ ). Using the Karhunen-Loève expansion (see e.g.[18]), the permeability fields can be expanded in terms of deterministic orthogonal basis  $\Phi_{j,s}(x)$  functions satisfying

$$\int_{\Omega} R_s(x_1, z_1; x_2, z_2) \Phi_{j,s}(x_2, z_2) dx_2 dz_2 = \lambda_{j,s} \Phi_{j,s}(x_1, z_1), \quad (7)$$

for  $j = 1, 2, \dots$ , where  $\lambda_{j,s} = E[Y_{j,s}^2] > 0$ . In turn, each permeability field is written as

$$Y_s(x, \omega) = \sum_{j=1}^{\infty} \sqrt{\lambda_{j,s}} \theta_{j,s}(\omega) \Phi_{j,s}(x), \quad (8)$$

where  $\theta_{j,s}$  denotes the random coefficients of the Karhunen-Loève expansion, and  $\lambda_{j,s}$  denotes the eigenvalues where as before,  $s$  is either  $m$  or  $f$ .

Due to the energy decay property of the correlation function, truncation of (8) into the first few terms corresponding to the dominant eigenvalues would in effect reduce the dimension of our uncertainty space. In the present work, each permeability field uses 20 eigenvalues for the Karhunen-Loève expansion (KLE). Fig. 1 illustrates the decline in eigenvalue size as the horizontal axis increases. In particular, by  $j = 20$  (the 20th eigenvalue for the matrix and

fracture) we see that the values have nearly vanished. From this point onward, we assume that uncertainty in the permeability fields have been parametrized by the random vectors  $\theta_m$  (for matrix) and  $\theta_f$  (for fracture), each belonging to  $\mathbb{R}^{20}$  and is associated with the coefficients in the KLE.

#### 4. MsFVEM and Iterative Decomposition

In this section we describe the Multiscale Finite Volume Element method (MsFVEM) to solve (1) that reflects a significant reduction in the computational load while at the same time maintaining a reasonable accuracy level. The basic problem is defined as follows. The permeability is defined on the underlying fine grid. We denote by  $\mathcal{K}^h$  the set of coarse elements  $K$ . We let  $\xi$  denote a coarse nodal point on the grid, and let  $V_\xi$  denote the associated coarse control volume. The pressure solutions are then computed on the coarse nodal points of the discretization. See Fig. 2 for a schematic of the coarse grid overlay on the underlying fine grid. The main idea is to incorporate the fine

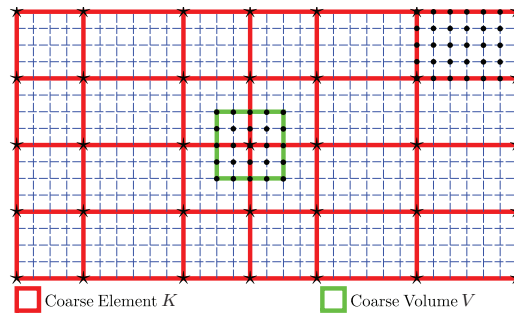


Figure 2: Schematic of the coarse grid overlay on the underlying fine grid

scale information of the underlying permeability description into a set of multiscale basis functions and express the pressure as their linear combination. The technique applied here follows the multiscale finite element method in [12], as the basis functions are determined from the solution of the leading order homogeneous elliptic equation on each coarse element. For a coarse rectangular element  $K$ , the basis functions  $\varphi_{i,K}^m$  ( $i = 1, \dots, 4$ ) and  $\varphi_{i,K}^f$  ( $i = 1, \dots, 4$ ) are computed from the governing equations

$$\begin{aligned} -\nabla \cdot (k_m(x, \theta_m) \nabla \varphi_{i,K}^m) &= 0 \quad \text{in } K & \text{and} & & -\nabla \cdot (k_f(x, \theta_f) \nabla \varphi_{i,K}^f) &= 0 \quad \text{in } K \\ \varphi_{i,K}^m &= g_i \quad \text{on } \partial K, & & & \varphi_{i,K}^f &= g_i \quad \text{on } \partial K, \end{aligned} \quad (9)$$

for a prescribed boundary function  $g_i$ . Here we assume that the uncertain vectors  $\theta_m$  and  $\theta_f$  are fixed. The boundary value problems in (9) must be solved four times for the determination of the four  $\{\varphi_{i,K}^m, \varphi_{i,K}^f\}$ . The basis function associated with the coarse nodal point  $\xi_i$  is constructed from the union of the basis functions that share this  $\xi_i$  and are zero elsewhere. Once the multiscale basis functions are formed, we seek the approximate pressures  $p_m^h$  and  $p_f^h$  in

$$V_m^h = \text{span} \{ \varphi_{i,K}^m : i = 1, \dots, 4, \quad K \in \mathcal{K}^h \} \quad \text{and} \quad V_f^h = \text{span} \{ \varphi_{i,K}^f : i = 1, \dots, 4, \quad K \in \mathcal{K}^h \},$$

respectively, such that

$$\begin{cases} \int_{V_\xi} \frac{\alpha k_m}{\mu} (p_m^h - p_f^h) dx - \int_{\partial V_\xi} \frac{k_m}{\mu} \nabla p_m^h \cdot \mathbf{n} dl = \int_{V_\xi} q_{m,p} dx \\ - \int_{V_\xi} \frac{\alpha k_m}{\mu} (p_m^h - p_f^h) dx - \int_{\partial V_\xi} \frac{k_f}{\mu} \nabla p_f^h \cdot \mathbf{n} dl = \int_{V_\xi} q_{f,p} dx \end{cases} \quad (10)$$

for every coarse control volume  $V_\xi$ .

The formulation described earlier yields a linear algebraic system

$$B_m P_m - B_f P_f + A_m P_m = Q_m \quad \text{and} \quad -(B_m P_m - B_f P_f) + A_f P_f = Q_f, \quad (11)$$

where  $P_m$  and  $P_f$  are the vectors of the unknown matrix and fracture pressures,  $Q_m$  and  $Q_f$  are the vectors resulting from integration of the forcing terms,  $A_m$  and  $A_f$  are matrices resulting from the boundary integral in (10), and  $B_m$  and  $B_f$  are matrices whose entries are

$$(B_m)_{ij} = \int_{V_i} \frac{\alpha k_m}{\mu} \varphi_j^m dx \quad \text{and} \quad (B_f)_{ij} = \int_{V_i} \frac{\alpha k_m}{\mu} \varphi_j^f dx.$$

In order to solve (11) we apply an iteration

$$(A_m + B_m)P_m^{(l)} = Q_m + B_f P_f^{(l-1)} \quad \text{followed by} \quad (A_f + B_f)P_f^{(l)} = Q_f + B_m P_m^{(l)}, \quad (12)$$

starting with an initial guess  $P_f^{(0)}$ . We note that similar approach has been used in [5]. We perform the iteration until we obtain a convergent solution pair  $(P_f^{(N)}, P_m^{(N)})$ , which for simplicity we denote by  $(P_f, P_m)$ . After each iteration we compute a summed relative error

$$E^{(l)} = \frac{\|P_m^{(l)} - P_m^{(l-1)}\|_{L_2(\Omega)}}{\|P_{m0}\|_{L_2(\Omega)}} + \frac{\|P_f^{(l)} - P_f^{(l-1)}\|_{L_2(\Omega)}}{\|P_{f0}\|_{L_2(\Omega)}}, \quad (13)$$

where  $\|\cdot\|_{L_2(\Omega)}$  denotes the spatial  $L_2$ -norm and  $P_{m0}$  and  $P_{f0}$  denote the matrix and fracture solutions in the case when there is no transfer term. The iteration is stopped when  $E^{(l)}$  reaches a pre-defined tolerance.

## 5. Stochastic sparse interpolation technique

Next we propose an alternative of using stochastic collocation for the multiscale basis function computations. This method involves a one-time preprocessing step of computing the basis functions,  $\varphi_{i,s}(x, \theta_s^k)$ , at  $N_c$  sparse points  $\{\theta_s^k\}_{k=1}^{N_c}$  in the uncertainty space. Then, rather than recomputing  $\varphi_{i,s}(x, \theta_s)$  for each realization  $\theta_s$ , we may use the interpolant

$$\varphi_{i,s}(x, \theta_s) = \sum_{k=1}^{N_c} \varphi_{i,s}(x, \theta_s^k) \alpha_k(\theta_s) \quad (14)$$

to obtain the multiscale basis functions associated with  $\theta_s$ . As before, the notation  $s$  refers to either matrix ( $m$ ) or fracture ( $f$ ). When the coefficients (i.e., interpolation weights)  $\alpha_k(\theta_s)$  are easily computable, the sparse grid interpolant proves to be a more efficient way to gain the basis functions.

The one-dimensional Lagrange interpolant of an arbitrary function  $g$  is defined as

$$U_i(g)(\theta) = \sum_{j=1}^{M_i} g(\theta_j^i) L_j^i(\theta), \quad \text{with} \quad L_j^i(\theta) = \prod_{k \neq j} \frac{(\theta - \theta_k^i)}{(\theta_j^i - \theta_k^i)} \quad (15)$$

being the usual Lagrange basis functions and  $M_i$  is the number of nodes in the  $i^{\text{th}}$  dimension. The full tensor interpolation in  $d$  dimensions is then given by

$$(U_{i_1} \otimes \cdots \otimes U_{i_d})(g) = \sum_{j_1=1}^{M_{i_1}} \cdots \sum_{j_d=1}^{M_{i_d}} g(\theta_{j_1}^{i_1}, \dots, \theta_{j_d}^{i_d}) \cdot (L_{j_1}^{i_1} \otimes \cdots \otimes L_{j_d}^{i_d}). \quad (16)$$

We note that for a moderate dimension, the number of terms in (16) makes this interpolation infeasible to compute. Rather than using a full tensor product interpolation in  $d$  dimensions, we use the Smolyak algorithm as an efficient sparse grid alternative [16]. Letting  $|\mathbf{i}| = i_1 + \cdots + i_d$  for  $\mathbf{i} \in \mathbb{N}^d$ , the Smolyak algorithm is defined by

$$A(q, d)(g) = \sum_{q-d+1 \leq |\mathbf{i}| \leq q} (-1)^{q-|\mathbf{i}|} \cdot \binom{d-1}{q-|\mathbf{i}|} \cdot (U_{i_1} \otimes \cdots \otimes U_{i_d})(g). \quad (17)$$

Most notably, we only need to evaluate the function  $g$  at sparse values given by

$$H(q, d) = \bigcup_{q-d+1 \leq |i| \leq q} (\Theta_{i_1} \otimes \cdots \otimes \Theta_{i_d}), \quad (18)$$

where  $\Theta_i = \{\theta_1^i, \dots, \theta_{M_i}^i\}$  are the fixed points used by  $U_i$ . In this work, we use interpolation points that are based on the extrema of Chebyshev polynomials [4].

## 6. Markov chain Monte Carlo method (MCMC)

At this stage, we are in a position to proceed with the actual procedure for sampling the matrix and fracture permeability fields which are conditioned to the available tracer cut data, denoted by  $F^{\text{ref}}(t)$ . We note that the map from the permeability fields to the tracer cut data is not one-to-one. Thus, this is an ill-posed inverse problem due to the fact that there exist many different permeability samples that will produce  $F^{\text{ref}}(t)$ . Within the statistical framework, we view the problem as taking the samples from the conditional distribution  $P((k_m, k_f)|F^{\text{ref}})$ . For brevity we now use  $F$  in the place of  $F^{\text{ref}}$ , and use  $k$  to denote a sample pair  $(k_m, k_f)$ . Bayes' theorem gives the relation

$$P(k|F) \propto P(F|k)P(k), \quad (19)$$

where  $P(k)$  denotes the prior distribution of the permeability field,  $P(F|k)$  denotes the likelihood function, and represents the conditional probability that the outcome of the measurement is  $F$  when the true permeability is  $k$ . We note that the likelihood function requires the forward solution of the flow problem, and in turn, accounts for the bulk of the computational cost for each permeability sample. This is the juncture at which we employ the MsFVEM combined with the sparse interpolation technique described earlier to calculate the simulated  $F_k(t)$  for a proposed  $k$ . For actual sampling from the posterior distribution  $P(k|F)$  we will be using the Metropolis-Hasting MCMC method [15].

As mentioned before, given a permeability sample  $k$ , we may obtain the tracer cut curve  $F_k$  through solving the model equations found in (1) and (2). The resulting  $F_k$  will contain error from both the model itself, and from the numerical scheme(s) used to solve the model. A viable assumption is the combined errors from measurement, modeling, and numerical schemes satisfy a Gaussian distribution [10]. In other words, we may write

$$P(F|k) \propto \exp\left(-\frac{\|F - F_k\|^2}{\sigma_f^2}\right), \quad (20)$$

where  $F$  is the observed tracer cut,  $F_k$  is the tracer cut obtained through solving (1) and (2) for a given  $k$ , and  $\sigma_f^2$  is the precision associated  $F$  and  $F_k$ . Noting that  $F$  and  $F_k$  are time dependent, the  $L^2$ -norm  $\|F - F_k\|^2$ , may be written

$$\|F - F_k\|^2 = \int_0^T (F(t) - F_k(t))^2 dt.$$

From (19), we may then write the posterior distribution as

$$P(k|F) \propto \exp\left(-\frac{\|F - F_k\|^2}{\sigma_f^2}\right) P(k). \quad (21)$$

The main idea of MCMC is to generate a Markov chain whose stationary distribution is given by  $P(k|F)$ . At each iteration a permeability pair  $k$  is proposed using a transitional probability distribution  $q(k|k_n)$ , where  $k_n$  denotes the previously accepted permeability sample. The forward problem is then solved to determine the acceptance probability

$$p(k_n, k) = \min\left(1, \frac{q(k_n|k)P(k|F)}{q(k|k_n)P(k_n|F)}\right).$$

More specifically,  $k_{n+1} = k$  with probability  $p(k_n, k)$  and  $k_{n+1} = k_n$  with probability  $1 - p(k_n, k)$ . The Metropolis-Hasting MCMC algorithm is summarized in Algorithm 1 [15].



**Algorithm 1** Collocation MsFVEM and Metropolis-Hasting MCMC

---

Given covariance structure, generate the KLE parametrization.

Compute the multiscale basis functions for predefined collocation points.

**for**  $n = 1$  to  $N_{\text{mcmc}}$  **do**

At state  $k_n$ , generate  $k$  from  $q(k|k_n)$ .

With  $k$  as input, solve the dual model to get the simulated  $F_k$ .

Accept  $k$  as a sample with probability

$$p(k_n, k) = \min \left( 1, \frac{q(k_n|k)P(k|F)}{q(k|k_n)P(k_n|F)} \right),$$

i.e., take  $k_{n+1} = k$  with probability  $p(k_n, k)$  and  $k_{n+1} = k_n$  with probability  $1 - p(k_n, k)$ .

**end for**

---

## 7. Numerical results

In this section we present a number of representative simulation results for tracer flow in the dual porosity, dual permeability system. We consider a two-dimensional square domain  $\Omega = [0, 1] \times [0, 1]$ . We impose Dirichlet conditions  $p_{m,L} = p_{f,L} = 1$  and  $p_{m,R} = p_{f,R} = 0$  on the left and right boundaries, respectively, and no flow (zero Neumann) conditions on the top and bottom portions of the boundary in (1). We use the initial conditions  $C_m(x, 0) = C_f(x, 0) = 1$  on the left boundary, and zero elsewhere for the tracer equations in (2). The matrix and fracture porosities are  $\phi_m = 0.7$  and  $\phi_f = 0.2$ , respectively. We use  $\alpha = 4$  as the shape factor. The tolerance for the error in (13) is fixed at  $1.0 \times 10^{-8}$  for all simulations.

The permeability fields are projected to a  $256 \times 256$  mesh in  $\Omega$ . In our simulation, the matrix permeability employs  $l_{x,m} = l_{z,m} = 0.1$  and variance  $\sigma_m^2 = 1$ , while the fracture permeability uses correlation lengths  $l_{x,f} = 0.9$ ,  $l_{z,f} = 0.04$  and variance  $\sigma_f^2 = 4$ . The dual pressure equations are solved by MsFVEM and the iterative decomposition on a  $16 \times 16$  mesh. The concentration equations are solved on the same  $16 \times 16$  mesh using a non-oscillatory explicit finite difference scheme with the minmod limiter.

Before embarking on the MCMC, it is worthwhile to see the performance of the sparse interpolation technique described earlier. With 20 dimensions, and a level 1 interpolation, we use 61 sparse grid points. Table 1 shows the difference between pressures computed by traditional MsFVEM and by collocation MsFVEM quantified in both the  $L_2$ -norm and  $H_1$ -norm. These pressures are computed for several realizations of  $(\theta_m, \theta_f)$ . The results in this table confirm the robustness of the sparse interpolation technique in Section 5.

We run MCMC with 5000 permeability proposals, and consider an independent sampler from a uniform distribution on  $[-1, 1]^{20}$  for the transitional probability distribution  $q(k|k_n)$ . The left plot of Fig. 3 shows the tracer cut curves obtained from the accepted permeabilities, while the right plot shows the norm of their differences against the reference tracer cut curve. Fig. 4 shows typical profiles of accepted permeability fields. We observe the same situation between the traditional and collocation MsFVEM. To emphasize this further, Fig. 5 compares the performance of MCMC for the traditional MsFVEM and collocation MsFVEM in terms of the probability density function of several entries of accepted  $\theta$ . We can see that both methods exhibit the same density functions.

In addition to the demonstrated accuracy of collocation MsFVEM, we also address the efficiency of the method. For all time comparisons we use the same dual-core machine equipped with two 2.66 GHz Intel Core i7 processors, each with 4GB of RAM. The traditional MsFVEM simulation results in a computational time of roughly 12–13 hours, whereas for the collocation MsFVEM simulation, we obtain a final computational time of roughly 9.5 hours. This is approximately a 27% saving in computation. However, we further remark on the savings associated with the basis function computations in (9). We emphasize that the basis function computations are the operations which distinguish traditional MsFVEM from collocation MsFVEM. All other computations are common between each respective method. For collocation MsFVEM we obtain a basis function computational time of 1.8 hours, in addition to a negligible pre-processing time of 2 minutes. This is in sharp contrast to the 4.7 hours which are spent on the basis function computations for traditional MsFVEM. In particular, when singling out the basis computations we encounter a computational saving of 62%. We expect that further optimization may lead to a more pronounced increase in efficiency,



yet these results adequately demonstrate the expected boost in efficiency associated with the collocation MsFVEM approach.

8. Concluding remarks

In this paper we have proposed a technique for characterizing a fractured porous medium through the use of a surrogate model for dual porosity, dual permeability tracer flow. We describe the Markov chain Monte Carlo (MCMC) procedure to sample the posterior distribution of the permeabilities of the surrogate model conditioned to available tracer cut data. To make computation more tractable, we propose the use of MsFVEM and a sparse interpolation technique as part of the model reduction techniques. The simulations which we present indicate promising results, and warrant a more detailed investigation in this direction.

Table 1: Comparison of pressure difference

$(\theta_m, \theta_f)$	Matrix		Fracture	
	$L_2$ (%)	$H_1$ (%)	$L_2$ (%)	$H_1$ (%)
1	0.05	0.06	0.13	0.06
2	0.04	0.05	0.06	0.03
3	0.04	0.04	0.03	0.01
4	0.03	0.04	0.07	0.03
5	0.11	0.15	0.06	0.06

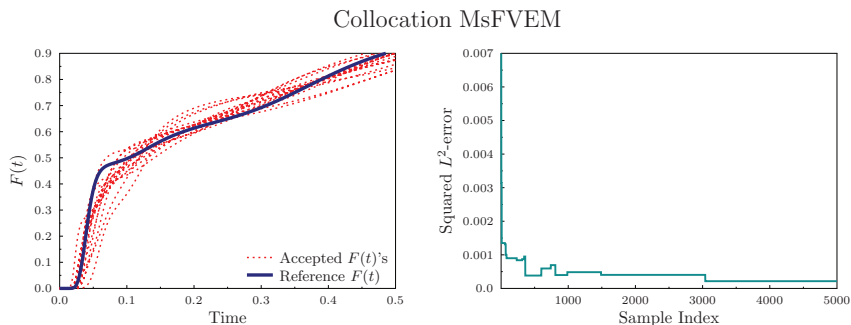


Figure 3: Tracer cut curves associated with the accepted permeability fields (left) and their deviation from the reference production (right)

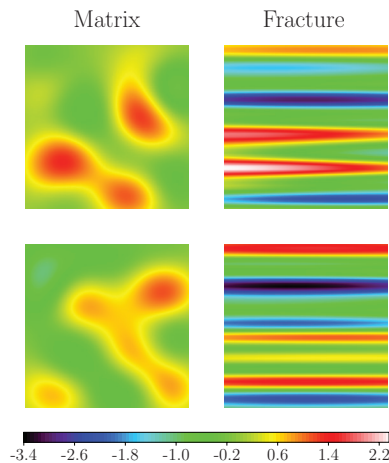
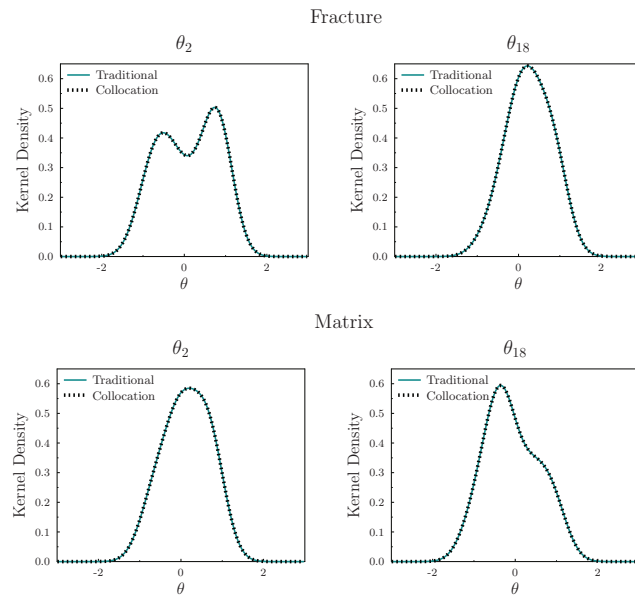


Figure 4: Typical profiles of accepted permeability fields

Figure 5: Comparison of probability density functions for several  $\theta$ 

**Acknowledgements** V. Ginting is supported in part by grants from US Department of Energy (DE-FE0004832 and DE-SC0004982), the Center for Fundamentals of Subsurface Flow of the School of Energy Resources of the University of Wyoming (WYDEQ49811GNTG and WYDEQ49811PER), and the National Science Foundation (DMS-1016283).

## References

- [1] T. Arbogast, "Analysis of the simulation of single phase flow through a naturally fractured reservoir", *SIAM J. Math. Anal.*, 26, 1989, 12–29.
- [2] T. Arbogast, J. Douglas, U. Hornung, "Derivation of the double porosity model of single phase flow via homogenization theory", *SIAM J. Math. Anal.*, 21(4), 1990, 823–836.
- [3] G. Barenblatt, I. Zheltov, I. Kochina, "Basic concepts in the theory of seepage of homogeneous liquids in fissured rocks [strata]", *SMM*, 24(5), 1960, 852–864.
- [4] V. Barthelmann, E. Novak, K. Ritter, "High dimensional polynomial interpolation on sparse grids", *Advances in Computational Mathematics*, 12, 2000, 273–288.
- [5] E. Choi, T. Cheema, M. Islam, "A new dual-porosity/dual-permeability model with non-Darcian flow through fractures", *J. Petrol. Sci. Eng.*, 17, 1977, 331–344.
- [6] P. Dostert, Y. Efendiev, T.Y. Hou, "Multiscale finite element methods for stochastic porous media flow equations and application to uncertainty quantification", *Comput. Methods Appl. Mech. Engrg.*, 197, 2008, 3445–3455.
- [7] B. Ganapathysubramanian, N. Zabaras, "Modeling diffusion in random heterogeneous media: Data-driven models, stochastic collocation and the variational multiscale method", *J. Comput. Phys.*, 226, 2007, 326–353.
- [8] J. Douglas, T. Arbogast, "Dual-porosity models for flow in naturally fractured reservoirs", *Dynamics of Fluids in Hierarchical Porous Media*, Academic Press, London, 1990, 177–221.
- [9] Y. Efendiev, A. Datta-Gupta, V. Ginting, X. Ma, B. Mallick, "An efficient two-stage Markov chain Monte Carlo method for dynamic data integration", *Water Resour. Res.*, 41, W12423, 2005.
- [10] Y. Efendiev, T. Hou, W. Luo, "Preconditioning Markov chain Monte Carlo simulations using coarse-scale models", *SIAM J. Sci. Comput.*, 28(2), 2006, 776–803.
- [11] D. Gamerman, "Markov Chain Monte Carlo. Stochastic Simulation for Bayesian Inference.", Chapman & Hall, Boca Raton, Florida, 1997.
- [12] T. Hou, X. Wu, "A multiscale finite element method for elliptic problems in composite materials and porous media", *J. Comput. Phys.*, 134, 1997, 169–189.
- [13] H. Kazemi, L. Merrill, K. Porterfield, P. Zeman, "Numerical simulation of water-oil flow in naturally fractured reservoirs", *SPE* 5719, 1976, 317–326.
- [14] A. Lange, J. Bouzian, B. Bourbiaux, "Tracer-test simulation on discrete fracture network models for the characterization of fractured reservoirs", *SPE*, 94344, 2005.
- [15] C. Robert, G. Casella, "Monte Carlo Statistical Methods", Springer-Verlag, New York, 1999.
- [16] S. A. Smolyak, "Quadrature and interpolation formulas for tensor products of certain classes of functions", *Soviet Math. Dokl.*, 4, 1963, 240–243.
- [17] J. Warren, P. Root, "The behavior of naturally fractured reservoirs", *SPE*, 426, 1963, 245–255.
- [18] E. Wong, "Stochastic Processes in Information and Dynamical Systems", McGraw-Hill, New York, 1971.